Organic Electronics 39 (2016) 199–206

Contents lists available at ScienceDirect

Organic Electronics

journal homepage: www.elsevier.com/locate/orgel

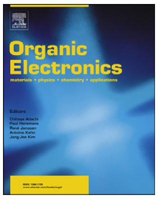

All-polymer phototransistors with bulk heterojunction sensing layers of thiophene-based electron-donating and thienopyrroledione-based electron-accepting polymers

Sungho Nam [a, b, c], Hwajeong Kim [a, d], Donal D.C. Bradley [b, c, **], Youngkyoo Kim [a, *]

[a] Organic Nanoelectronics Laboratory, Department of Chemical Engineering, School of Applied Chemical Engineering, Kyungpook National University, Daegu 41566, Republic of Korea
[b] Department of Physics, Division of Mathematical, Physical and Life Sciences, University of Oxford, Oxford OX1 3PD, United Kingdom
[c] Department of Engineering Science, Division of Mathematical, Physical and Life Sciences, University of Oxford, Oxford OX1 3PD, United Kingdom
[d] Priority Research Center, Research Institute of Advanced Energy Technology, Kyungpook National University, Daegu 41566, Republic of Korea

ARTICLE INFO

Article history:
Received 26 May 2016
Received in revised form
28 September 2016
Accepted 30 September 2016

Keywords:
All-polymer phototransistor
Polymer/polymer bulk heterojunction
Edge-on
Responsivity
Lateral charge transport

ABSTRACT

All-polymer phototransistors consisting of bulk heterojunction (BHJ) nanolayers of electron-donating (p-type) and electron-accepting (n-type) polymers are attractive candidates for applications such as light-sensing and light-switching devices. Here, we report efficient green-light-sensing all-polymer phototransistors based on BHJ layers of poly(3-hexylthiophene) (P3HT) and poly[(4,8-bis(2-ethylhexyloxy)-benzo[1,2-*b*:4,5-*b*]-dithiophene)-2,6-diyl-*alt*-(*N*-2-ethylhexylthieno[3,4-*c*]pyrrole-4,6-dione)-2,6-diyl]] (PBDTTPD) polymers. To understand the phototransistor characteristics, all devices were exposed to a green monochromatic light (555 nm) with different incident power intensities. The results showed that the P3HT:PBDTTPD (80:20) layer are more advantageous than the pristine P3HT layers in terms of efficient charge separation and transport. The responsivity value of devices with the P3HT:PBDTTPD (80:20) layers reached 33.3 A/W, which is 25 and 28 times higher than those obtained with pristine the pristine P3HT or P3HT:PBDTTPD (60:40) layers. The enhanced device performance of the P3HT:PBDTTPD (80:20) phototransistors is attributable to an efficient charge separation, prevalent edge-on chain orientation, and relatively smoother surface morphology, which might facilitate improved charge transport in the lateral direction.

1. Introduction

Organic optoelectronic devices, such as organic light-emitting diodes, organic field-effect transistors, organic solar cells, organic optical memory devices and organic photodetectors, have attracted great attention because of their advantages over inorganic counterparts in terms of the suitability for large-area/flexible modules and the inexpensive low-temperature fabrication utilizing various printing techniques [1–7]. In particular, organic photodetectors have great potentials for bendable optical sensors in the flexible electronic devices and biomedical applications including artificial eyes and optical coherence tomography [8–10]. Of various types of organic photodetectors, organic phototransistors (OPTRs) have advantages in signal amplification and active-matrix modulation due to their device geometry with three electrodes, compared to organic photodiodes with two electrodes [11–14].

Interestingly, most OTPRs have employed single p-type (electron-donating) or n-type (electron-accepting) materials as a channel layer, even though blends of p-type and n-type materials can deliver much higher sensitivity owing to efficient exciton dissociation by the bulk heterojunction (BHJ) concept [15–17]. The BHJ-type OPTRs can be fabricated with blend films of polymers and small molecules, as well understood from the polymer/fullerene solar cells [18–20]. However, the stability and durability of devices cannot be well supported by the polymer/small molecule BHJ films because small molecules have disadvantages such as migration and recrystallization leading to aggregations during long time operations [21–23].

On this account, all-polymer phototransistors have been

---

[*] Corresponding author.
[**] Corresponding author. Department of Physics, Division of Mathematical, Physical and Life Sciences, University of Oxford, Oxford OX1 3PD, United Kingdom.
E-mail addresses: donal.bradley@mpls.ox.ac.uk (D.D.C. Bradley), ykimm@knu.ac.kr (Y. Kim).

http://dx.doi.org/10.1016/j.orgel.2016.09.034
1566-1199/

introduced by employing both p-type and n-type polymers without any small molecules [24,25]. The previous reports demonstrated that all-polymer phototransistors can be efficiently operated even in the presence of the large amount of n-type polymer components. In particular, near infrared (NIR) light could be successfully detected by all-polymer phototransistors with the BHJ channel layers that contain n-type polymers featuring broadband optical absorptions [26]. However, thienopyrroledione-based polymers have not been used as an n-type polymer component for all-polymer phototransistors even though they have polar carbonyl groups leading to excellent electron-accepting characteristics.

In this study, we fabricated all-polymer phototransistors by employing the BHJ films of p-type poly(3-hexylthiophene) (P3HT) and n-type poly[(4,8-bis(2-ethylhexyloxy)-benzo[1,2-*b*:4,5-*b*]-dithiophene)-2,6-diyl-*alt*-(*N*-2-ethylhexylthieno[3,4-*c*]pyrrole-4,6-dione)-2,6-diyl]] (PBDTTPD) polymers. The phototransistor performances were examined by varying incident light intensities (P_{IN}) at a fixed wavelength of ~555 nm, taking into consideration the strong optical absorption in the visible region. The corrected responsivity (R_C), was extracted from the transistor performances under illumination by removing the dark current of transistors. The BHJ (P3HT:PBDTTPD) layers were investigated with synchrotron radiation grazing-incidence angle X-ray diffraction (GIXD) and atomic force microscopy (AFM) in order to understand the correlation between the BHJ nanostructure/surface morphology and the device performance.

2. Experimental section

2.1. Materials and solutions

Regioregular P3HT polymer (weight-average molecular weight = 30 kDa, polydispersity index, PDI = 1.7, regioregularity > 97%) was purchased from Rieke Metals, Inc.; the PBDTTPD polymer (weight-average molecular weight = 130 kDa, PDI = 2.5) was received from Solarmer Materials, Inc., and the poly(methyl methacrylate) (PMMA) polymer (weight-average molecular weight = 120 kDa, PDI = 2.2) was supplied by Sigma-Aldrich. Solutions of pristine and binary blend solutions of the two polymers (P3HT:PBDTTPD = 100:0, 80:20, and 60:40 by weight) were prepared using toluene at a solid concentration of ca. 10 mg/mL. The PMMA powder was dissolved in *n*-butyl acetate at a solid concentration of 80 mg/mL. All solutions were subjected to vigorous stirring on a magnetic stirring plate for 48 h before spin coating.

2.2. Device fabrication

Indium-tin oxide (ITO)-coated glass substrates were patterned using a photolithography/etching process, to make 1 mm × 12 mm stripes for use as gate electrodes. The patterned ITO-coated glass substrates were cleaned using acetone and isopropyl alcohol in an ultrasonic bath, and dried with nitrogen flow. The PMMA gate-insulating layers (~600 nm) were spin-coated on the ITO-coated glass substrates and soft-baked at 60 °C for 15 min, followed by annealing at 120 °C for 15 min. Next, the pristine P3HT and P3HT:PBDTTPD BHJ layers (40–50 nm) were spin-coated on top of the PMMA layers and soft-baked at 60 °C for 15 min. All samples were transferred into a vacuum chamber inside an argon-filled glove box. After pumping down the chamber pressure to ~1×10^{-6} torr, Ni (~10 nm) and Al (~70 nm) were sequentially deposited on top of the pristine/BHJ layers through a shadow mask, to form source-drain electrodes with 2-mm channel widths and 70-μm channel lengths. Finally, all samples were subjected to thermal annealing at 120 °C for 30 min.

2.3. Measurements and analysis

The film thickness was measured using a surface profiler (Alpha Step 200, Tencor Instruments). The optical absorption and photoluminescence spectra of the pristine and BHJ layers were measured using a UV-visible spectrometer (Optizen 2120, MECASYS) and a PL spectrometer (FS-2, SCINCO), respectively. The transistor characteristics of all devices were measured using a semiconductor analyser (Keithley 2636B). The incident light wavelength was controlled with a monochromator (CM110, Spectral Products), from the white light generated by a tungsten-halogen lamp (150 W, ASBN-W, Spectral Products) and neutral density filters, and the incident light intensity (P_{IN}) was calibrated with a Si photodiode (818-UV, Newport, USA). The nanostructure of the pristine and BHJ layers was examined using a synchrotron radiation GIXD system (X-ray wavelength = 0.12479 nm, incidence angle = 0.12°, 3C SAXS I beamline, Pohang Accelerator Laboratory). The surface morphologies of the film samples were measured using AFM (Nanoscope IIIa, Digital Instruments).

3. Results and discussion

The P3HT:PBDTTPD phototransistors were fabricated using a typical bottom-gate and top-contact transistor structure (see Fig. 1a). We first investigated the optical absorption and photoluminescence (PL) spectra of the used polymers. As shown in Fig. 1b, both P3HT and PBDTTPD polymers showed strong optical absorption in the visible region. The optical density of the blend (P3HT:PBDTTPD) films in the wavelength of 550–650 nm increased gradually as the PBDTTPD content increased because of the dominant absorption of the PBDTTPD polymer (555–680 nm). Considering the energy offset of the highest occupied molecular orbital (HOMO) and lowest unoccupied molecular orbital (LUMO) energy levels of the two polymers (~0.6 eV for ΔE_{HOMO} and ~0.7 eV for ΔE_{LUMO}), we can expect a sufficiently large driving force for efficient charge separation from the excitons generated in both the P3HT and PBDTTPD domains (note that the HOMO and LUMO energy levels were obtained by photoelectron yield spectra (PEYS) and calculated from the HOMO and the optical band gap energy of the two polymers, respectively (see Figs. S1 and S2)) [27,28]. The PL quenching (with an excitation wavelength of 555 nm) of the P3HT:PBDTTPD BHJ layer does not depend on the blend composition, as can be seen in Fig. 1c; this shows that a charge separation/transfer process between the P3HT and PBDTTPD polymers through Förster energy transfer has occurred. We note here that the PL intensity of the pristine P3HT and PBDTTPD polymers is higher than that of the two different P3HT:PBDTTPD blend films (80:20 and 60:40) [29,30].

We first examined the basic device performance of the pristine P3HT and all-polymer (P3HT:PBDTTPD) transistors under dark conditions (see Fig. 2a and b). All devices exhibited a typical hole-dominant (p-type) behaviour, as results from their output and transfer curves. We should note that an electron-dominant behaviour could not be obtained regardless of the blend composition ratio, because of the large electron injection barrier from the Ni electrode to the LUMO level of the PBDTTPD polymer; not even a hole-dominant behaviour in the pristine PBDTTPD thin film could be obtained (see Figs. S3 and S4). Interestingly, the P3HT:PBDTTPD (80:20) blend films exhibited a device performance comparable to that of the pristine P3HT film with respect to the drain current (I_D), whereas a significant reduction in I_D was observed in the P3HT:PBDTTPD (60:40) blend films. As the PBDTTPD content increased, the threshold voltage (V_{TH}) increased considerably, from −13.9 V for the pristine P3HT film to −21.7 and −22.8 V for the